Correlating molecule count and release kinetics with vesicular size using open carbon nanopipettes

Keke Hu,† Rui Jia,§ Amir Hatamie,† Kim Long Le Vo,† Michael V. Mirkin§ and Andrew G. Ewing†,*

† Department of Chemistry and Molecular Biology, University of Gothenburg, Kemivägen 10, 41296 Gothenburg, Sweden;

§ Department of Chemistry and Biochemistry, Queens College-CUNY, Flushing, NY 11367, USA.

Supporting Information Placeholder

ABSTRACT: In this work open carbon nanopipettes (CNPs) with radius between 50 nm and 600 nm were used to control translocation of different size vesicles through the pipette orifice followed by nanoelectrochemical analysis. Vesicle impact electrochemical cytometry (VIEC) was used to determine the number of catecholamine molecules expelled from single vesicles onto an inner wall carbon surface where the duration of transmitters release was quantified and correlated to vesicle size all in the same nanotip. This in turn allows us to both size and count molecules for vesicles while in a living cell. Here, small and sharp open CNPs were employed to carry out intracellular vesicle impact electrochemical cytometry (IVIEC) with minimal invasion and high sensitivity. Our findings with VIEC reveal that vesicular content increases with vesicle size. Release kinetics of vesicular transmitters and dense core size have the same relation with vesicle size, implying that vesicular dense core size determines speed of each release event. This direct correlation unravels one of the complexities of exocytosis.

Exocytosis is the key process for cell-to-cell communication in endocrine cells and neurons. It is mediated by neurotransmitter release from nanometer sized secretory vesicles. These vesicles can be roughly divided into two main types according to their size and different components, small synaptic vesicles (SSVs) and large dense core vesicles (LDCVs). SSVs are smaller types and appear clear under TEM images. LDCVs contain two compartments, one fast compartment called the halo with soluble and freely moving transmitters and the other slow compartment of a protein core with bound transmitters. [1-4] LDCVs are present in a number of biological systems. Adrenal chromaffin cells, the widely used model system for exocytosis studies, contain a great number of LDCVs making up 30% of total cellular volume.[5]

The amount of catecholamine molecules inside a vesicle is one of the regulators that affect exocytosis.[6] It's imperative to obtain vesicular content to understand regulation mechanisms of exocytosis. In 2009 Omiatek et al. combined capillary electrophoresis and microfluidics with electrochemical detection to quantify vesicular content.[7] Later, Dunevall et al. characterized content of mammalian vesicles by direct absorption and rupture of vesicles on 33 μm diameter disk-shaped carbon electrodes, a technique termed VIEC. [8] After that, several studies were carried out aiming at understanding the potential mechanisms regarding vesicle opening and rupturing on the surface of the electrodes during VIEC. [9-12]

In addition to vesicular content, quantification of transmitter concentration in individual vesicles and correlation between vesicular size and content is important for comprehensive understanding of the mechanisms of exocytosis. Very recently, Zhang et al. reported quantification of vesicular size and catecholamine content at the same time by combination of resistive pulse measurements with VIEC to calculate catecholamine concentration of single chromaffin vesicles, providing quantitative information about the vesicle maturation process.[13] Pan et al. have shown that using open CNPs translocation of single liposomes and release of loaded dopamine can be monitored simultaneously.[14]

Another aspect that could be influential in exocytotic regulation is the speed or temporal regulation of release events. It has been suggested that release of transmitters bound to proteins filled inside dense core could be delayed due to their slower diffusion into the extracellular space.[15-16] Lovrić et al. combined TEM with NanoSIMS images of a single vesicle and distinguished distribution of labeled dopamine across dense core and halo. Correlating imaged amounts of dopamine in vesicles obtained from NanoSIMS with those from electrochemical methods, they concluded that dopamine loading/unloading between dense core and halo solution is a kinetically limited process, revealing both loading of messengers and release into and out of the nanometer protein dense core with a time scale on the order of hours.[17]

The development of above methodologies has enriched our knowledge of fundamental mechanisms of exocytosis, yet much remains unknown, especially the correlation between vesicular structure and release dynamics. Carbon nanopipettes (CNPs) prepared by chemical vapor deposition (CVD) of carbon into pre-pulled quartz nanopipettes have proven to be applicable to electroactive transmitter detection.[18-19] After modification with Pt black, they were also employed in measurements of reactive oxygen and nitrogen species inside single organelles and vesicles.[20-21] In this paper, we have controlled orifice size of open CNPs in VIEC measurement, distribution of $N_{molecules}$ was correlated with vesicle size. The general trend of vesicular content and release kinetics over vesicle size was obtained. Comparing variations of release kinetics and dense

core size according to vesicle size, direct connection between speed of release event and dense core size was created. Finally, we demonstrate a measurement of combined IVIEC and vesicle size with an open CNP in a living cell.

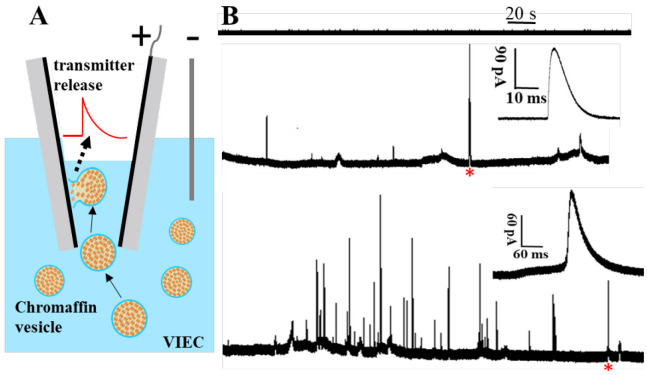

Figure 1. VIEC measurement with different size open CNPs. Schematic of VIEC measurement in homogenizing buffer with open CNPs (A) and representative amperometric traces of 100, 200 and 400 nm radius open CNPs (from top to bottom) at 700 mV vs Ag/AgCl, inset shows amplified spikes labeled with red asterisk (B).

Figure 1A shows a schematic of the VIEC measurement with an open CNP. Sizes of single vesicles allowed to diffuse into the infinite cavity were under control by adjusting CNPs size (TEM images of CNPs are shown in Figure S1). Oxidation of messenger molecules from single vesicles bursting on the electrode inside the nanotip results in a current transient at the CNP. Representative amperometric traces recording the content of individual vesicles are presented in Figure 1B. Altogether 8 radii of CNPs were used including 50, 100, 200, 250, 300, 400, 500 and 600 nm. Amperometric traces of 50 and 100 nm CNPs gave no spikes indicating essentially no vesicles below 100 nm radius (Figure 3B), consistent with results from TEM images. Current transients mostly with smaller I_{max} and time duration started to be observed from 200 nm CNPs coming from rupture of vesicles between 100 nm and 200 nm while at 400 nm CNPs a larger number of bursts were captured. (Additional amperometric traces of CNPs are shown in Figure S2). Important information about the release event can be obtained by analyzing the individual spikes. The number of electroactive molecules expelled from individual vesicles can be quantified based on Faraday's law, $N_{molecules}=N_A Q/nF$, where N_A is Avogadro's number, Q is the charge calculated by integration of current over time of individual spikes, n is number of electron transferred during oxidation reaction ($2e^-$ for catecholamines) and F is the Faraday constant. The number of catecholamine molecules ($N_{molecules}$) corresponding to each spike of different size CNPs was quantified and is presented in normalized frequency histograms in Figure 2.

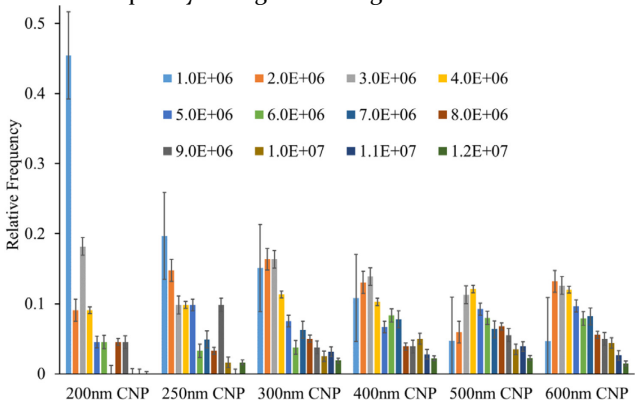

Figure 2. Normalized frequency histograms of $N_{molecules}$ obtained from different size open CNPs (200,250, 300, 400, 500 and 600 nm radius). (Bin size, 1×10^6 molecules, collected from 4 isolation of adrenal chromaffin vesicles, 98 open CNPs were used)

Markedly different ratios of $N_{molecules}$ of 1×10^6 across different size CNPs are shown in Figure 2. For vesicles smaller than 200 nm, vesicles containing 1×10^6 transmitters make up 45% of total vesicles, this ratio keeps decreasing as vesicle size increases up to 500 nm. And the largest $N_{molecules}$ for vesicles below 200 nm is within 9×10^6, quite different from their counterparts. The ratio of vesicles with larger content of transmitters generally increases with vesicle size. For vesicles below 250 nm, vesicles with lowest amount of 1×10^6 transmitters account for the biggest percentage and that ratio decreases with vesicular content while for larger ones, the frequency of vesicles first goes up and then goes down with peak mostly appearing at contents of 2×10^6 and 3×10^6 as $N_{molecules}$ increases. It should be noted that there is a slight change in distribution from 500 to 600 nm CNPs, implying that the size of a small number of vesicles are above 500 nm. This can be further confirmed by comparing averages of vesicular content and release kinetics between 500 and 600 nm CNPs in Figure 3A and results from TEM imaging in Figure 3B.

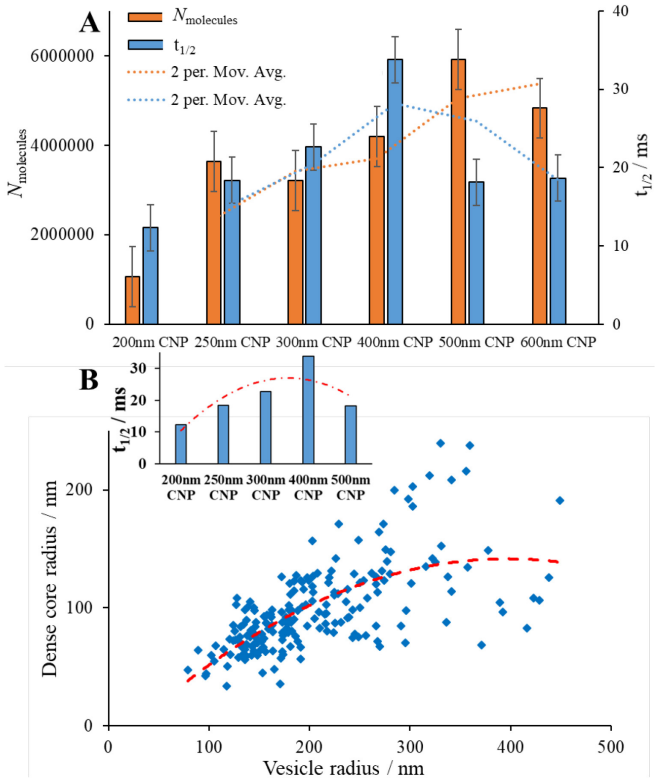

Figure 3. Correlation of vesicular content and release kinetics with vesicle size. Histograms of average $N_{molecules}$ and $t_{1/2}$ derived from different sizes open CNPs with trend lines (2 period moving average) (A) and TEM data on vesicle dimensions with trend line (2 order polynomial). Inset shows histogram of $t_{1/2}$ for 200 to 500 nm open CNPs with trend line (2 order polynomial) (B). ($N_{molecules}$ and $t_{1/2}$ are medians obtained from each size of open CNPs, specific numbers are listed in Table S1. Dense core radius and vesicle radius was measured from TEM images of chromaffin cells (Figure S4))

As shown in Figure 3A, from 200 to 500 nm CNPs, average vesicular content increases with vesicle size and this makes sense considering distribution of $N_{molecules}$ over size in Figure 2. Apart from $N_{molecules}$, duration of messenger release ($t_{1/2}$),

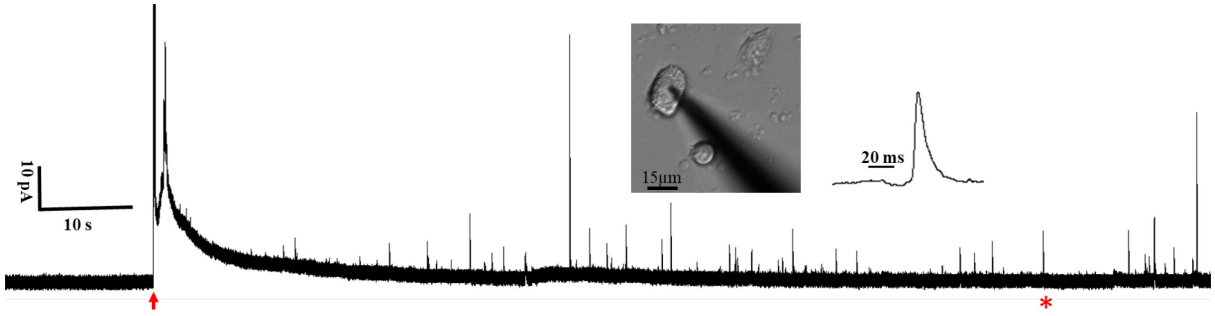

Figure 4. Representative amperometric trace of IVIEC measurement with a 400 nm radius open CNP at 700 mV vs. Ag/AgCl. Inset shows image of a CNP being inserted into an 18 μm diameter chromaffin cell during IVIEC measurement and amplified spike labeled with red asterisk. (The red arrow indicated the moment the CNP was pushed through the cell membrane)

time needed for fusion pore to open (t_{rise}) and oxidation of vesicular content or pore to close again (t_{fall}) can also be quantified by analyzing individual current transients.[22] Release kinetics versus vesicle size is presented in Figure 3A with similar numbers for 500 and 600 nm CNPs. In contrast to the trend line of vesicular content, the duration of chemical messenger release first increases with vesicle size and peaks at 400 nm CNPs, and beyond that decreases substantially. The same trends of t_{rise} and t_{fall} are presented in Figure S3. As discussed before, aggregated protein in the vesicular dense core can slow down release of chemical messengers.[15-16] It is possible that changes in release kinetics are related to dense core size. By measuring dense core size from TEM images of chromaffin cells (Figure S4), dense core size over vesicle size was obtained. The trend line in Figure 3B shows that dense core size increases with vesicle size within ~380 nm, whereas after that dense core size drops significantly and almost all the points are below the trend line. Although the data are somewhat scattered at the larger sizes, there is a corresponding trend with the change in release kinetics (see inset in Figure 3B). We conclude that the kinetics of chemical messenger release is limited by dense core size.

In addition to VIEC, open CNPs were used to carry out IVIEC of vesicles in a living cell. Figure 4 presents an amperometric trace of the IVIEC measurement inside an 18 μm diameter chromaffin cell with a 400 nm radius CNP. The red arrow indicates the moment the CNP was pushed through the cell membrane. After a slight vibration, the CNP was inserted inside with reasonable background current at 700 mV. After IVIEC measurements, both 18-μm and 13-μm diameter chromaffin cells maintained no observable morphological changes, (Figure S5 and S6) suggesting minimized disruption of intracellular environment and cell function. For intracellular use, it is crucial for biological cells to maintain their integrity and viability. Although tip size of CNPs is relatively large compared to the commonly used nano-tip carbon fiber microelectrodes in IVIEC measurements,[23-24] here only a small portion of tip end pierced into cytoplasm allowing vesicles together with cytosol to be driven into pipettes by capillary action or diffusion. As can be seen from the amperometric trace in Figure 4, increased frequency of rupture events was observed about 25 seconds after CNP was inserted inside. For intracellular electrochemical analysis with nanoelectrodes, trade-offs between scale and sensitivity have been the main issue that need to be addressed. Despite the small tip size, the hollow structure of CNPs provides a sufficiently large electrochemical area for oxidation of vesicular transmitters and this is also critical for in vivo measurement in small organisms.

In conclusion, we present a combination of VIEC with open CNPs for characterization of chemical messengers in single vesicles entering and impacting the electrode in the CNP. With this new method, correlation of vesicle content and release kinetics with vesicle size can be obtained. Our results demonstrate that the speed of release events depends on vesicular dense core size. Direct correlation between vesicular structure and release dynamics was established and this will offer new insights into regulation of exocytosis, including an unprecedented ability to study the effect of dense core matrix dissociation on release kinetics. Besides application in VIEC, open CNPs with smaller physical size and larger electroactive surface area are promising for in situ intracellular test and potential for in vivo measurement inside small organisms such as *Drosophila*, zebra fish etc.

ASSOCIATED CONTENT

Supporting Information. Experimental details, TEM images of CNPs, additional amperometric traces of CNPs, medians of $N_{molecules}$ and $t_{1/2}$ at different size of CNPs, histograms of t_{rise} and t_{fall}, TEM images of chromaffin cells, including Figures S1 – S6 and Table S1. This material is available free of charge via the Internet at http://pubs.acs.org.

AUTHOR INFORMATION

Corresponding Author
*andrewe@chem.gu.se

Notes
The authors declare no competing financial interests.

ACKNOWLEDGMENT

We acknowledge funding from the European Research Council (Advanced Grant), the Knut and Alice Wallenberg Foundation, the Swedish Research Council (VR), the National Institutes of Health. AH specifically acknowledges support from Sweden's Innovation Agency (Vinnova) and the Swedish Strategy Group for EU-coordination. MVM acknowledges the support by the National Science Foundation (CHE-1763337).

REFERENCES

1. Huttner, W. B.; Gerdes, H. H.; Rosa, P., The granin-(chromogranin/secretogranin) family. Trends Biochem. Sci **1991**, 16, 27-30.
2. Wiedenmann, B.; Huttner, W. B., Synaptophysin and chromogranins/secretogranins widespread constituents of distinct types of neuroendocrine vesicles and new tools in tumor diagnosis. Virchows Archiv B **1989**, 1, 95-121.

3. Oleinick, A.; Hu, R.; Ren, B.; Tian, Z.-Q.; Svir, I.; Amatore, C., Theoretical Model of Neurotransmitter Release during In Vivo Vesicular Exocytosis Based on a Grainy Biphasic Nano-Structuration of Chromogranins within Dense Core Matrixes. J. Electrochem. Soc. **2015**, 4, H3014-H3024.
4. Yao, J.; Erickson, J. D.; Hersh, L. B., Protein Kinase A Affects Trafficking of the Vesicular Monoamine Transporters in PC12 Cells. Traffic **2004**, 12, 1006-1016.
5. Plattner, H.; Artalejo, A. R.; Neher, E., Ultrastructural Organization of Bovine Chromaffin Cell Cortex—Analysis by Cryofixation and Morphometry of Aspects Pertinent to Exocytosis. J. Cell Biol. **1997**, 7, 1709-1717.
6. Pothos, E.; Desmond, M.; Sulzer, D., l-3,4-Dihydroxyphenylalanine Increases the Quantal Size of Exocytotic Dopamine Release In Vitro. J. Neurochem. **1996**, 2, 629-636.
7. Omiatek, D. M.; Santillo, M. F.; Heien, M. L.; Ewing, A. G., Hybrid Capillary-Microfluidic Device for the Separation, Lysis, and Electrochemical Detection of Vesicles. Anal. Chem. **2009**, 6, 2294-2302.
8. Dunevall, J.; Fathali, H.; Najafinobar, N.; Lovric, J.; Wigström, J.; Cans, A.-S.; Ewing, A. G., Characterizing the Catecholamine Content of Single Mammalian Vesicles by Collision–Adsorption Events at an Electrode. J. Am. Chem. Soc. **2015**, 13, 4344-4346.
9. Lovrić, J.; Najafinobar, N.; Dunevall, J.; Majdi, S.; Svir, I.; Oleinick, A.; Amatore, C.; Ewing, A. G., On the mechanism of electrochemical vesicle cytometry: chromaffin cell vesicles and liposomes. Faraday Discuss. **2016**, 0, 65-79.
10. Li, X.; Dunevall, J.; Ren, L.; Ewing, A. G., Mechanistic Aspects of Vesicle Opening during Analysis with Vesicle Impact Electrochemical Cytometry. Anal. Chem. **2017**, 17, 9416-9423.
11. Li, X.; Ren, L.; Dunevall, J.; Ye, D.; White, H. S.; Edwards, M. A.; Ewing, A. G., Nanopore Opening at Flat and Nanotip Conical Electrodes during Vesicle Impact Electrochemical Cytometry. ACS Nano **2018**, 3, 3010-3019.
12. Najafinobar, N.; Lovrić, J.; Majdi, S.; Dunevall, J.; Cans, A. S.; Ewing, A., Excited Fluorophores Enhance the Opening of Vesicles at Electrode Surfaces in Vesicle Electrochemical Cytometry. Angew. Chem. Int. Ed. Engl. **2016**, 48, 15081-15085.
13. Zhang, X.-W.; Hatamie, A.; Ewing, A. G., Simultaneous Quantification of Vesicle Size and Catecholamine Content by Resistive Pulses in Nanopores and Vesicle Impact Electrochemical Cytometry. J. Am. Chem. Soc. **2020**, 9, 4093-4097.
14. Pan, R.; Hu, K.; Jiang, D.; Samuni, U.; Mirkin, M. V., Electrochemical Resistive-Pulse Sensing. J. Am. Chem. Soc. **2019**, 50, 19555-19559.
15. Montesinos, M. S.; Machado, J. D.; Camacho, M.; Diaz, J.; Morales, Y. G.; Alvarez de la Rosa, D.; Carmona, E.; Castañeyra, A.; Viveros, O. H.; O'Connor, D. T.; Mahata, S. K.; Borges, R., The Crucial Role of Chromogranins in Storage and Exocytosis Revealed Using Chromaffin Cells from Chromogranin A Null Mouse. J. Neurosci. **2008**, 13, 3350-3358.
16. Helle, K. B.; Reed, R. K.; Pihl, K. E.; Serck-Hanssen, G., Osmotic properties of the chromogranins and relation to osmotic pressure in catecholamine storage granules. Acta Physiol. Scand. **1985**, 1, 21-33.
17. Lovrić, J.; Dunevall, J.; Larsson, A.; Ren, L.; Andersson, S.; Meibom, A.; Malmberg, P.; Kurczy, M. E.; Ewing, A. G., Nano Secondary Ion Mass Spectrometry Imaging of Dopamine Distribution Across Nanometer Vesicles. ACS Nano **2017**, 4, 3446-3455.
18. Hu, K.; Wang, D.; Zhou, M.; Bae, J. H.; Yu, Y.; Xin, H.; Mirkin, M. V., Ultrasensitive Detection of Dopamine with Carbon Nanopipets. Anal. Chem. **2019**, 20, 12935-12941.
19. Yang, C.; Hu, K.; Wang, D.; Zubi, Y.; Lee, S. T.; Puthongkham, P.; Mirkin, M. V.; Venton, B. J., Cavity Carbon-Nanopipette Electrodes for Dopamine Detection. Anal. Chem. **2019**, 7, 4618-4624.
20. Hu, K.; Li, Y.; Rotenberg, S. A.; Amatore, C.; Mirkin, M. V., Electrochemical Measurements of Reactive Oxygen and Nitrogen Species inside Single Phagolysosomes of Living Macrophages. J. Am. Chem. Soc. **2019**, 11, 4564-4568.
21. Pan, R.; Hu, K.; Jia, R.; Rotenberg, S. A.; Jiang, D.; Mirkin, M. V., Resistive-Pulse Sensing Inside Single Living Cells. J. Am. Chem. Soc. **2020**, 12, 5778-5784.
22. Mosharov, E. V.; Sulzer, D., Analysis of exocytotic events recorded by amperometry. Nature Methods **2005**, 9, 651-658.
23. Li, X.; Majdi, S.; Dunevall, J.; Fathali, H.; Ewing, A. G., Quantitative Measurement of Transmitters in Individual Vesicles in the Cytoplasm of Single Cells with Nanotip Electrodes. Angew. Chem. Int. Ed. **2015**, 41, 11978-11982.
24. Yue, Q.; Li, X.; Wu, F.; Ji, W.; Zhang, Y.; Yu, P.; Zhang, M.; Ma, W.; Wang, M.; Mao, L., Unveiling the Role of DJ-1 Protein in Vesicular Storage and Release of Catecholamine with Nano/Micro-Tip Electrodes. Angew. Chem. Int. Ed. Engl. **2020**, 27, 11061-11065

TOC Graphic

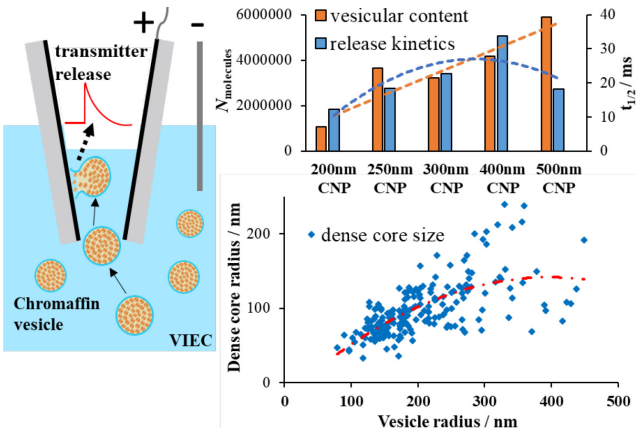
+
-
transmitter release
Chromaffin vesicle
VIEC
vesicular content
release kinetics
$N_{molecules}$
$t_{1/2}$ / ms
6000000
4000000
2000000
0
40
30
20
10
0
200nm CNP
250nm CNP
300nm CNP
400nm CNP
500nm CNP
dense core size
Dense core radius / nm
200
100
0
0
100
200
300
400
500
Vesicle radius / nm